Published in final edited form as:

J Immunol. 2015 August 1; 195(3): 1242–1250. doi:10.4049/jimmunol.1500243.

KIR3DS1 specific D0 domain polymorphisms disrupt KIR3DL1 surface expression and HLA binding[1]

Tiernan J. Mulrooney[*], **Aaron C. Zhang**[*], **Yehuda Goldgur**[†], **Jeanette E. Boudreau**[*], and **Katharine C. Hsu**[*,‡,§]

[*]Department of Immunology, Memorial Sloan Kettering Cancer Center, New York, New York, United States of America

[†]Department of Structural Biology, Memorial Sloan Kettering Cancer Center, New York, New York, United States of America

[‡]Department of Medicine, Memorial Sloan Kettering Cancer Center, New York, New York, United States of America

[§]Weill Medical College, Cornell University, New York, New York, United States of America

Abstract

KIR3DL1 is a polymorphic inhibitory receptor that modulates natural killer cell activity through interacting with HLA-A and HLA-B alleles that carry the Bw4 epitope. Amino acid polymorphisms throughout KIR3DL1 impact receptor surface expression and affinity for HLA. *KIR3DL1/S1* encodes inhibitory and activating alleles, but despite high homology with KIR3DL1, the activating receptor KIR3DS1 does not bind the same ligand. Allele *KIR3DL1*009* resulted from a gene recombination event between the inhibitory receptor allele *KIR3DL1*001* and the activating receptor allele *KIR3DS1*013*. This study analyzed the functional impact of KIR3DS1-specific polymorphisms on KIR3DL1*009 surface expression, binding to HLA, and functional capacity. Flow cytometric analysis of primary human NK cells as well as transfected HEK293T cells show that KIR3DL1*009 is expressed at a significantly lower surface density compared to KIR3DL1*001. Using recombinant proteins of KIR3DL1*001, KIR3DL1*009, and KIR3DS1*013 to analyze binding to HLA, we found that while KIR3DL1*009 displayed some evidence of binding to HLA compared to KIR3DS1*013, the binding was minimal compared to KIR3DL1*001 and KIR3DL1*005. Mutagenesis of polymorphic sites revealed that the surface phenotype and reduced binding of KIR3DL1*009 are caused by the combined amino acid polymorphisms at positions 58 and 92 within the D0 extracellular domain. Resulting from these effects, KIR3DL1*009-positive NK cells exhibited less inhibition by HLA-Bw4 positive target cells compared to KIR3DL1*001-positive NK cells. The data from this study contribute novel insight into how KIR3DS1-specific polymorphisms in the extracellular region impact KIR3DL1 surface expression, ligand binding, and inhibitory function.

[1]This work was supported by the National Institutes of Health Grants AI069197, CA023766, and HL088134.

Corresponding author: Katharine C. Hsu, MD, PhD, Phone: 646-888-2667, Fax: 646-422-0298, hsuk@mskcc.org.

Introduction

Natural killer cells are lymphocytes of the innate immune system that are important for the host immune defense against viral pathogens and malignant cells. NK cells are capable of cytotoxic function and can also secrete cytokines that stimulate the adaptive immune system (1, 2). In contrast to T and B lymphocytes, NK cells do not express antigen specific receptors, but rather express a variety of activating and inhibitory receptors, including the killer immunoglobulin-like receptors (KIR). Activation of NK cells is modulated by a balance of signaling events induced by these receptors at the immune synapse (3). Many of the inhibitory receptors, including KIR, recognize HLA as a marker of "self" to prevent NK cell mediated auto-reactivity (4, 5). As virally infected cells or malignant cells down-regulate HLA on the cell surface to evade the adaptive immune system, these cells become more susceptible to NK cell-mediated lysis (6, 7).

The polymorphic *KIR* gene family is located on human chromosome 19q13.4 and encodes both inhibitory and stimulatory receptors that are stochastically expressed by NK and T cells. The *KIR* genes encode type I integral membrane proteins that contain either three (KIR3D) or two extracellular (KIR2D) Ig-like domains. In general, KIR with a long cytoplasmic tail (KIR3DL and KIR2DL) containing two ITIMs function as inhibitory receptors; upon recognition of self-HLA molecules (8–10), the phosphatases SHP1 and SHP2 are recruited to the ITIMs, resulting in the induction of inhibitory signaling (11, 12). In addition to inhibition, the interaction between KIR and HLA is vital to determining the activation potential of an NK cell. Through a mechanism referred to as "licensing" or "education," NK cells that express an inhibitory KIR for a cognate self-HLA molecule display a lower threshold for activation and a greater functional response to target cells (13, 14).

Nearly all individuals are positive for the *KIR3DL1/S1* gene (15, 16). *KIR3DL1* encodes an inhibitory receptor that binds to HLA-A and HLA-B molecules that carry the Bw4 epitope designated by amino acid residues 77, 80–83 in the alpha-1 helix of HLA (17–19). Polymorphisms in the extracellular domains between KIR3DL1 and KIR3DS1 are relatively limited, yet KIR3DS1 demonstrates a unique surface expression profile compared to KIR3DL1 and, with the exception of the rare KIR3DS1*014, is unable to bind HLA-Bw4 (20). The KIR3DL1 alleles have developed extensive diversification through gene recombination events and point mutations. *KIR3DL1*009*, which is found in 2% of the general population, is a product of a gene conversion event involving the common inhibitory allele *KIR3DL1*001* and a 1.5 kb sequence of the common activating allele *KIR3DS1*01301* which contains the exons that encode the D0 extracellular domain (21, 22). Resulting from this conversion, *KIR3DL1*009* is identical to *KIR3DL1*001* both upstream and downstream of this *KIR3DS1*01301* insert. KIR3DL1*009 presents a unique opportunity to determine the critical polymorphic residues within the D0 domain that affect ligand recognition and the surface phenotype of KIR3DL1/S1. We demonstrate that the combined polymorphisms at amino positions 58 and 92 within the D0 domain of KIR3DL1*009 result in reduced surface expression and ligand binding compared to KIR3DL1*001. We further show that these polymorphic residues impact other KIR3DL1 alleles, as KIR3DL1*042 which resulted from a conversion between KIR3DS1*013 and

KIR3DL1*005 also demonstrates reduced binding to HLA. These findings provide further molecular mechanisms that can explain the lack of reactivity between KIR3DS1*013 and HLA-Bw4 and contributes new data that can help understand the impact of the KIR/HLA interaction on clinical outcomes.

Materials and methods

Peripheral blood lymphocytes and cell lines

Primary peripheral blood mononuclear cells (PBMCs) were collected anonymously from buffy coats obtained from the New York Blood Center (NYBC, New York, NY), where donors provided written informed consent. Additional consent from these donors was waived by the MSKCC IRB. All PBMCs were cryopreserved prior to experimental analysis. PBMCs were thawed and cultured overnight in RPMI 1640 supplemented with 250 units/ml IL-2. The parental, HLA-A,B,C negative 721.221 cell line as well as 721.221 cells stably expressing HLA-B*44:03 were kind gifts from Dr. Carolyn K. Hurley (Georgetown University, Washington, DC, USA) and were maintained in RPMI 1640. The human embryonic kidney cell line, HEK293T, was maintained in DMEM. All media used to maintain the primary cells and cells lines described above were supplemented with 10% fetal bovine serum, 1 mM L-glutamine, 10 mM HEPES buffer, and 1 mM sodium pyruvate. The Expi293F cell line was cultured in the proprietary Expi293 Expression medium as recommended by the manufacturer (Life Technologies, Carlsbad, CA, USA).

DNA constructs

The cDNA encoding *KIR3DL1*001* was a kind gift of Dr. Daniel McVicar (National Cancer Institute, Bethesda, MD, USA). The *KIR3DL1*001* cDNA was cloned in the pcDNA3-Clover plasmid (a kind gift from Dr. Michael Lin, Addgene plasmid 40259) upstream and in-frame with the Clover cDNA (23). The stop codon was mutated to create a C-terminally tagged full-length KIR molecule. Constructs encoding *KIR3DL1*005KIR3DL1*009*, and *KIR3DL1*001* mutants were created via site-directed mutagenesis as previously described with the modification of using Platinum high fidelity Taq (Life Technologies) and associated buffers (24). To generate KIR-Fc constructs, cDNA consisting of the IL-2 signal peptide, exons encoding the extracellular domains of KIR3DL1*001 and the Fc region of human IgG1 was cloned into the mammalian expression vector pCDNA3.4. All other KIR-Fc constructs were created via site-directed mutagenesis. All constructs were prepared as per manufacturer's instructions using the HiSpeed Plasmid Maxi Kit (Qiagen, Valencia, CA, USA). The cDNA sequences were confirmed by the MSKCC DNA Sequencing Core Facility (New York, NY, USA).

KIR3DL1*009 screening

DNA from the NYBC donors was isolated using the Qiagen DNeasy Blood and Tissue kit. Donors were first screened using PCR methods previously described to identify donors potentially positive for *KIR3DL1*009* (21, 25, 26). DNA samples from donors identified as positive for *KIR3DL1*009* by PCR were subsequently evaluated by sequencing as previously described (27).

KIR3DL1 surface expression

Receptor expression was detected on the surface of primary NK cells (CD56+, CD3−) following staining of PBMCs with the KIR3DL1 specific antibodies, DX9 (BD Biosciences, Franklin Lakes, NJ, USA) and Z27 (Beckman Coulter, Brea, CA, USA), conjugated to PE and APC, respectively. To detect KIR3DL1 surface expression on HEK293T cells, 2×10^5 cells were transiently transfected with 1.0 μg of plasmids encoding the full-length cDNA of KIR3DL1 alleles under the control of a CMV promoter using the XtremeGENE HP DNA transfection reagent (Roche, Nutley, NJ, USA). Forty-eight hours post-transfection, KIR3DL1 surface expression was analyzed on viable, Clover-positive cells using the KIR3DL1 specific antibody, DX9. Surface expression data are presented as a ratio of KIR3DL1 surface expression (DX9 MFI) to total KIR3DL1 expression (Clover MFI). Flow cytometry experiments were assessed using an LSR Fortessa (BD Biosciences) and analyzed using FlowJo software version 9.7.6 (Treestar, Ashland, OR, USA).

KIR3DL1 internalization

The internalization of KIR3DL1 on transfected HEK293T cells was analyzed as previously described (28). Briefly, 16 hours post-transfection, the transfectants were probed with PE-conjugated DX9 and cultured at 37°C for 0, 20, 60 or 120 minutes. At each time point samples were either untreated or treated with an acidic solution (pH 2.5) containing 10 mM glycine to strip away externally bound antibodies. The amount of internalized receptor was analyzed by flow cytometry. The percentage of internalized KIR3DL1 was calculated using the following equation: $100 \times (MFI_{exp} - MFI_{zero})/(MFI_{total} - MFI_{zero})$. The MFI_{exp} represents the MFI of the internalized KIR3DL1 at a specific time point. The MFI_{total} and MFI_{zero} represent KIR3DL1 expression in samples either not treated with the acidic solution or samples stained with DX9 and immediately treated with the acid, respectively.

RNA isolation and RT-PCR

PBMC's were cultured overnight as above and probed with the KIR3DL1 specific antibody, DX9. The KIR3DL1 negative, low density and high density populations were sorted by the MSKCC Flow Cytometry Core Facility (New York, NY, USA). RNA was isolated from each population using the RNeasy Mini kit as per manufacturer's instruction (Quiagen) and converted to cDNA using the high capacity cDNA reverse transcription kit (Life Technologies). KIR3DL1*001 and KIR3DL1*009 were amplified using the respective forward primers, 5'-GCTATACAAAGAAGACAGAATCCACA-3' and 5'-CAAAGAAGACAGAATCCACG-3'. The reverse primer for both reactions was 5'-GGGAGCTGACAACTGATAGGG-3'. The conditions and control primers for each reaction have been previously described (21).

Production of soluble KIR-Fc recombinant proteins

To generate the soluble KIR-Fc proteins, Expi293F cells (7.5×10^7) were transfected with 30 μg of the appropriate plasmid using the Expifectamine 293F transfection reagent (Life Technologies) following the manufacturer's protocol. Seven days post-transfection, the supernatants containing the secreted recombinant proteins were harvested and the concentration of soluble KIR-Fc was determined using the Easy-titer human IgG assay

according to the manufacturer's protocol (Pierce Biotechnologies, Rockford, IL, USA). All recombinant proteins were analyzed for proper folding using conformation-specific antibodies, as described previously (29). Briefly, protein A coated microspheres (Bangs Laboratories, Fishers, IN, USA) were incubated with 1.0 μg of the KIR-Fc proteins for one hour at 4°C. KIR-Fc molecules were conformationally tested to determine that the recombinant proteins are folded similarly to how they are on the cell surface by flow cytometry using the conjugated KIR3DL1 conformational specific antibodies, DX9 and Z27 (Supplemental figure 1). As further confirmation of conformational specificity, recombinant KIR3DL1*001 was denatured at 70°C for two minutes prior to conjugation to the microspheres.

Detection of soluble KIR-Fc binding to HLA

The parental 721.221 cell line or 721.221 cells stably expressing HLA-B*44:03 (2×10^5) were incubated with either a single concentration (4.0 μg/ml) or a range of concentrations (0.4 – 4.0 μg/ml) of soluble KIR-Fc proteins for one hour at 4°C. The samples were washed twice with cold PBS, probed with a PE-conjugated goat antibody specific for human IgG (One Lambda, Canoga Park, CA, USA), and analyzed by flow cytometry. The KIR-Fc proteins were also tested for binding to a panel of single antigen HLA molecules conjugated to uniquely identifiable microspheres (One Lambda) as previously described in the presence of the blocking antibody, DX9 (4.0 μg/ml), or an isotype control (30). The KIR-Fc proteins (4.0 μg/ml) were incubated with 5 μl of beads for one hour at room temperature while rotating at 300 rpm. The beads were washed three times with wash buffer and probed with a PE-conjugated goat antibody specific for human IgG. The beads were washed twice with wash buffer and the samples were analyzed on a LABScan 100 using the Xponent software (Luminex, Austin, TX, USA). To account for potential variation of HLA density on each bead, the beads were probed with the PE-conjugated pan-HLA class I antibody, W6/32 (eBioscience, San Diego, CA, USA). The MFI values obtained for each interaction between KIR and HLA were first background subtracted for binding to the negative control bead, followed by normalization to the amount of HLA detected for each individual bead region.

CD107a mobilization assay

Following overnight culture in 10^3 U/mL IL-2, 5×10^5 PBMCs were co-incubated for four hours with either 5×10^4 parental 721.221 cells or 721.221 cells stably expressing HLA-B*44:03 in the presence of an APC H7 conjugated CD107a specific antibody (BD biosciences). To block inhibition imparted by the KIR3DL1, HLA-B*44:03 interaction, DX9 (20 μg/ml) was added to the co-incubation. Following this incubation, the cells were probed with conjugated antibodies specific for CD56 (Beckman Coulter), CD3 (Biolegend), KIR2DL2/L3 (BD Biosciences), KIR2DL1/S1 (Beckman Coulter), NKG2A (Beckman Coulter), ILT-2 (Beckman Coulter) and KIR3DL1 (Z27, Beckman Coulter). Using the differential surface expression phenotypes of the two KIR3DL1 alleles, the percent CD107a positive of each KIR3DL1 population was determined and adjusted for the percent CD107a positive of the KIR-/NKG2A- population to control for differences in the activation potential of the target cells. The data for each allele are expressed as a ratio comparing the degranulation responses observed against each target cell to the CD107a results observed following co-incubation with the HLA negative 721.221 cells.

Molecular modeling and simulations

A model of KIR3DL1*009 was based on the crystal structure of KIR3DL1*001-pHLA-B*5701 complex, PDB ID 3VH8 (31). A fragment of KIR3DL1 (residues 7 to 197) with mutations introduced by means of the interactive program O was subject to molecular dynamics simulation with Desmond/Maestro suite for 1.2 ns using the default parameters (neutralization with Cl^- ions, NaCl concentration 0.15 M, force field OPLS_2005, temperature 300 K, pressure 1.01 bar, Coulombic cutoff 9.0 A) (32).

Statistical analyses

All experiments were performed in triplicate and reproduced in at least two independent experiments. The results were analyzed as indicated by unpaired Student's t-test or by a one-way or two-way ANOVA followed by a Tukey's multiple comparisons test. Unless noted, the error bars in figures represent the standard error of the mean (SEM). All statistical analyses were performed with Graphpad Prism 6.0 software (La Jolla, CA, USA).

Results

KIR3DL1*009 is expressed at a low surface density

Amino acid polymorphisms amongst the KIR3DL1 alleles can impact the surface expression phenotype of the encoded receptor while the mRNA expression of these alleles remains similar (33, 34). *KIR3DL1*001* and *KIR3DL1*009* encode for receptors that differ by three amino acids, all of which lie within the D0 extracellular domain (Table I). We compared surface expression of KIR3DL1*009 to two KIR3DL1 allotypes with known high and low expression patterns. Constructs encoding *KIR3DL1*001KIR3DL1*005* or *KIR3DL1*009* fused C-terminally to the fluorescent protein, Clover, were transiently transfected into HEK293T cells. KIR3DL1 surface expression on Clover positive cells showed that the surface phenotype of KIR3DL1*009 was similar to KIR3DL1*005, which is known to be expressed at a low surface density (Figure 1A) (35). In contrast, KIR3DL1*009 surface expression was lower compared to the known high-density receptor, KIR3DL1*001. To control for total KIR3DL1 expression, the data are expressed as a ratio of KIR3DL1 surface expression (DX9 MFI) to total KIR expression within the Clover positive cells (Clover MFI) (Figure 1B). This quantification further illustrates the similarity in surface expression between KIR3DL1*009 and KIR3DL1*005 and the difference in surface expression observed between KIR3DL1*009 and KIR3DL1*001. The difference in surface expression is not due to differential affinity for the DX9 antibody as bead-conjugated recombinant KIR3DL1*001 and KIR3DL1*009 proteins similarly bound DX9 as determined by flow cytometry (Supplemental figure 1).

To identify which of the three amino acid polymorphisms contributes to the low surface expression phenotype of KIR3DL1*009, mutations were made to the construct encoding wild type *KIR3DL1*001*. Mutation constructs were created to encode receptors carrying each possible combination of the amino acid polymorphisms between KIR3DL1*001 and KIR3DL1*009. Surface expression of these mutant receptors along with wild type KIR3DL1*001 and KIR3DL1*009 were analyzed on transiently transfected HEK293T cells (Figure 1C). The individual polymorphisms at amino acid positions 47 (I47V) and 92

(V92M) had minimal impact on surface expression compared to wild type KIR3DL1*001. Similarly, these two polymorphisms (I47V, V92M) in combination, did not dramatically affect KIR3DL1*001 surface expression, although the addition of I47V appeared to restore the modest loss of surface expression associated with the single V92M mutant ($p < 0.001$). In contrast, a single change from serine to glycine at position 58 (S58G) caused a significant reduction in surface expression, comparable to that of the wild type KIR3DL1*009. When the S58G mutation was combined with V92M (S58G, V92M), surface expression remained significantly reduced. When the S58G mutation was combined with I47V (I47V, S58G), however, the reduction in surface expression was not as dramatic, further suggesting that the valine at position 47 helps to rescue surface expression. These results implicate the glycine at position 58 as the key polymorphism underlying the low surface expression of KIR3DL1*009 and suggest that the additional polymorphism at position 92 can counteract the rescuing effect imparted by the valine at position 47.

In these experiments, transcription of each allele was controlled by a CMV promoter, suggesting the lower surface expression of KIR3DL1*009 could be caused by amino acid polymorphisms that reduce surface stability or processing and trafficking of the receptor to the surface as observed with other KIR3DL1 and KIR2DL molecules (24, 36–38). To determine if the D0 polymorphisms impacted the surface stability of KIR3DL1*009, we monitored the internalization of the receptor on transfected HEK293T cells. We observed no difference in the internalization of KIR3DL1*009 compared to that of KIR3DL1*001 (Figure 1D). Therefore, we hypothesized that intracellular retention of KIR3DL1*009 caused the reduction in surface expression. Similar intracellular retention caused by improper folding of the receptor has been demonstrated for KIR3DL1*004 (39). At physiological temperatures, the allotype KIR3DL1*004 is not expressed at the cell surface. However, culturing cells transfected with this allele at sub-physiological temperatures resulted in detectable surface expression that was correlated with less intracellular retention of the receptor within the endoplasmic reticulum (ER) (39). To determine if KIR3DL1*009 is intracellularly retained in a similar fashion, KIR3DL1 surface expression was analyzed on transfected HEK293T cells following culture at either 37°C or 25°C (Figure 1D). As observed above, culture at 37°C results in a two-fold difference between KIR3DL1*009 and KIR3DL1*001 surface expression. However, when the transfectants were cultured at 25°C, KIR3DL1*009 surface expression increased to a level nearly equivalent to that observed for KIR3DL1*001.

Resulting from the surface expression differences observed in the transfection model, we analyzed KIR3DL1 surface expression on primary NK cells from healthy donors heterozygous for *KIR3DL1*001* and *KIR3DL1*009*. Two distinct KIR3DL1 positive NK cell populations were distinguishable using the KIR3DL1 specific antibodies, DX9 and Z27 (Figure 2A). To determine if KIR3DL1*001 and KIR3DL1*009 expression was segregated to specific populations, KIR3DL1 mRNA expression was analyzed in the KIR3DL1 negative, low density and high density populations using primers that specifically amplify either KIR3DL1*001 or KIR3DL1*009 (Figure 2B). These RT-PCR data reveal that KIR3DL1*001 and KIR3DL1*009 mRNA expression were detected exclusively in the high and low density KIR3DL1 populations, respectively, supporting the data from the

transfection model that KIR3DL1*009 is expressed at a lower density compared to KIR3DL1*001. Also, since the antibody clone DX9 is capable of binding the KIR3DL1*009 population on primary NK cells, these D0 polymorphisms are not responsible for the lack of DX9 binding to KIR3DS1. To further analyze surface expression of KIR3DL1 on primary NK cells, we compared the KIR3DL1 expression of the heterozygous KIR3DL1*001/KIR3DL1*009 to KIR3DL1 surface expression from donors expressing either KIR3DL1*001 or KIR3DL1*005 alone (Figure 2C). In accordance with previous reports, KIR3DL1*001 and KIR3DL1*005 donors exhibited high and low KIR3DL1 surface phenotypes, respectively. The flow cytometry analysis showed that the higher density population from the heterozygous donor matched the surface expression of the KIR3DL1*001 donors while the lower surface density population matched the phenotype of the KIR3DL1*005 donors. These data further support the findings from the transfection model that the polymorphisms present within KIR3DL1*009 cause the receptor to have a low surface phenotype that is similar to KIR3DL1*005.

Combined polymorphisms at amino acid position 58 and 92 result in poor binding to HLA

The polymorphisms within the D0 domain of KIR3DL1*009 are not predicted to directly interact with HLA and, to date, have not been examined for their role in ligand recognition. To understand if these polymorphisms impact the receptor's ability to interact with HLA, soluble KIR-Fc recombinant proteins containing the extracellular domains of KIR3DL1*009, KIR3DL1*001, KIR3DL1*042, KIR3DL1*005 or KIR3DS1*013 were analyzed by flow cytometry for binding to HLA-B*44:03 stably expressed on the surface of 721.221 cells (Figure 3A). KIR3DL1*042 and KIR3DL1*005 were analyzed as KIR3DL1*042 shares the D0 polymorphisms of KIR3DS1*013, but is identical to KIR3DL1*005 for the remainder of the mature protein (Table I). As expected, KIR3DS1*013 exhibited no binding to HLA. While KIR3DL1*009 and KIR3DL1*042 exhibited some evidence of binding to HLA-B*44:03 in comparison to KIR3DS1*013, the level of KIR3DL1*009 and KIR3DL1*042 binding was minimal compared to that of KIR3DL1*001 and KIR3DL1*005 (Figure 3B). KIR3DL1*005 exhibited enhanced binding to HLA-B*44:03 compared to KIR3DL1*001 which could be attributed to the polymorphic residue at position 283 (Figure 3B, Supplemental figure 2E) (40). The difference in binding to HLA-B*44:03 between KIR3DL1*001 and KIR3DL1*009 was consistent over a dose range of the KIR-Fc proteins (Figure 3C). To demonstrate specificity of binding, all of the KIR-Fc binding to HLA-B*44:03 on the surface of the cells could be blocked by DX9 and Z27 (Supplemental figure 2A-D).

To identify the residues that interfere with the interaction between KIR3DL1*009 and HLA, the construct encoding KIR3DL1*001-Fc was mutated to account for each combination of amino acid polymorphisms between KIR3DL1*001 and KIR3DL1*009. Binding of each of the mutant recombinant proteins to HLA-B*44:03 was compared to the binding of the wild type receptors (Figure 3D). Mutation of KIR3DL*001 at positions 47 (I47V) or 58 (S58G), independently or in combination (I47V, S58G), had minimal impact on the receptor's ability to bind HLA. However, the presence of a methionine at position 92 (V92M) resulted in a 60% reduction in binding to HLA compared to KIR3DL1*001. While the combination of valine at position 47 and methionine at position 92 (I47V, V92M) further decreased binding

compared to the single change at position 92 (V92M), the mutant still exhibited significantly more binding compared to the wild-type KIR3DL1*009. It was the combination of glycine at position 58 and methionine at position 92 (S58G, V92M) that reduced binding of HLA to levels comparable to that of KIR3DL1*009.

To examine if the reduced binding observed for KIR3DL1*009 and KIR3DL1*042 to HLA-B*44:03 was applicable to other HLA-Bw4 antigens, the wild-type recombinant KIR-Fc proteins as well as the mutant protein containing the combined polymorphisms at position 58 and 92 (S58G, V92M) were tested for binding to 23 different HLA Bw4 and 31 non-interacting HLA-Bw6 antigens presenting a heterogeneous pool of peptides using a bead-based multiplex platform (Figure 4). Consistent with the results for binding to HLA-B*44:03, the recombinant KIR3DL1*009 and KIR3DL1*042 showed significantly reduced binding to all HLA Bw4 molecules analyzed, compared to KIR3DL1*001 and KIR3DL1*005 (Figure 4A). Specificity of the KIR-Fc proteins is demonstrated as no binding to the HLA-Bw6 antigens was observed and the binding to the HLA-Bw4 antigens could be blocked by DX9. In support of the binding to HLA-B*44:03 on 721.221 cells, the presence of a glycine and methionine at positions 58 and 92, respectively, were responsible for the reduced binding of soluble KIR3DL1*009 to all of the HLA molecules tested (Figure 4B). These data further demonstrate that the diminished binding exhibited by KIR3DL1*009 and KIR3DL1*042 is broadly applicable for a large number of HLA molecules.

Molecular dynamic modeling of KIR3DL1*009 suggests 92M structurally impacts the conformation of KIR3DL1*009

We then sought to understand how the KIR3DL1*009 polymorphisms impact the structure and ligand interfaces between KIR and HLA. The polymorphic positions 47, 58 and 92 all reside outside of the direct KIR/HLA interface (Figure 5A) (31). Position 92, however, is located on the final strand (G) of the D0 domain that leads into the D1 domain. As V92M was identified as the key polymorphism that disrupts KIR3DL1*009 binding to HLA, we hypothesized this position may cause a conformational shift in the receptor that would indirectly impact the KIR/HLA interaction. To understand how the KIR3DL1*009 polymorphisms may impact the receptor structure, a molecular dynamic simulation was performed on the KIR3DL1*001 crystal structure following insertion of the KIR3DL1*009 polymorphisms (Figure 5B). Consistent with the binding data, the polymorphisms at positions 47 and 58 did not impact the overall structure of KIR3DL1. However, V92M caused a significant change in the structure likely resulting from steric hindrance caused by the bulkier side chain of methionine. Interestingly, the change in conformation did not appear to impact the interface between D0 and HLA even though the amino acids involved at this interface (9F, 11S, 13W) are on a neighboring strand (A). In contrast, V92M caused a dramatic conformational shift in the overall protein structure. In particular, the hinge angle between the D0 and D1 domains defined as the angle between Cα atoms of residues 82, 178 and 197 is 92° in the crystal structure of KIR3DL1*001, but measures 102° following the molecular dynamic simulation of KIR3DL1*009. This conformational change causes a significant displacement of the loops between the C and C’ strands as well as the E and F strands that contain the residues (138G, 140S, 165M, 166L, 167A) that directly interact with HLA. These data support the observed binding data, suggesting that the reduced capability

of KIR3DL1*009 to bind HLA is caused primarily by the polymorphism, V92M, which results in a conformational change of the D1 domain.

KIR3DL1*009 positive NK cells functionally respond against HLA-B*44:03 target cells

We then evaluated how the observed lower surface expression and weaker ligand binding might impact KIR3DL1*009 receptor function. CD107a mobilization was monitored on KIR3DL1 positive NK cells from a healthy donor heterozygous for *KIR3DL1*001* and *KIR3DL1*009* following incubation with HLA-negative 721.221 cells or 721.221 cells stably expressing HLA-B*44:03 in the presence or absence of the DX9 blocking antibody. Based on the differential surface expression phenotypes of these alleles determined by Z27 staining, degranulation by KIR3DL1*001 and KIR3DL1*009 populations could be independently monitored. This donor was not positive for an HLA-Bw4 antigen, thereby negating a potential effect of licensing differences between these two populations. Accordingly, the response levels as measured by CD107a mobilization, were equivalent between the KIR3DL1*001 and KIR3DL1*009 positive populations following stimulation with the HLA-negative 721.221 cells demonstrating that these two populations have equal thresholds for activation against target cells. Likewise, blocking the KIR3DL1, HLA-B*44:03 interaction with the DX9 antibody rescued the degranulation of each population to levels similar to the response against the HLA negative 721.221 cells (Figure 6). However, in the absence of a blocking antibody, the KIR3DL1*009-positive NK cells demonstrated significantly greater potential to degranulate compared to the KIR3DL1*001-positive NK cells when co-incubated with a HLA-Bw4 positive target cell. Activation of the KIR3DL1*009 positive population was two fold greater following co-incubation with HLA-Bw4 targets in the absence of the DX9 antibody compared to the activation response of the KIR3DL1*001 positive population. To understand if this enhanced ability to respond was due to lower surface expression or to reduced binding strength, inhibition of KIR3DL1*005 positive NK cells from a HLA-Bw4 negative individual was monitored in parallel. Degranulation of the KIR3DL1*005 population against the 721.221 targets was equal to the responses observed for the KIR3DL1*001 and KIR3DL1*009 populations. Similar to the KIR3DL1*001 population, the KIR3DL1*005 positive NK cells were inhibited significantly more by HLA-B*44:03 compared to the KIR3DL1*009 population. These data demonstrate that the reduced binding strength exhibited by KIR3DL1*009 allows the KIR3DL1*009-positive NK cells to maintain greater activation against a Bw4 positive target cell compared to KIR3DL1*001 and KIR3DL1*005.

Discussion

KIR3DL1 functions as an inhibitory receptor that recognizes HLA-A and HLA-B molecules that carry the Bw4 epitope (17–19). The *KIR3DL1/S1* gene has evolved under balancing selection into two distinct lineages of inhibitory KIR3DL1 allotypes and one lineage of activating KIR3DS1 allotypes (41). The two inhibitory receptors in this study, KIR3DL1*001 and KIR3DL1*009, segregate as members of the KIR3DL1*005-like lineage based on sequence homology (15). Differing from the extensive polymorphisms within the KIR3DL1 lineages, the KIR3DS1 allotypes have remained fairly conserved. Meiotic recombination events and mutations are the main contributors to the diversity of the

KIR3DL1 lineages. The two most common regions for recombination involve the D0 domain polymorphisms and a dimorphism at position 283 of the D2 domain. KIR3DL1*009 and KIR3DL1*042 resulted from such a genetic conversion event involving KIR3DS1*013 with either KIR3DL1*001 or KIR3DL1*005, respectively (22). Although the protein sequences of KIR3DL1*009 and KIR3DL1*042 are more similar to their KIR3DL1 parental alleles, the minimal HLA binding exhibited by these receptors is more analogous to that observed for KIR3DS1*013. The findings of this study provide novel insight into the functional consequences of KIR3DS1-specific D0 polymorphisms to explain the lack of binding between KIR3DS1*013 and HLA-Bw4.

The data from both primary NK cells and a transfection model revealed KIR3DL1*009 is expressed at a low surface density similar to the expression levels previously characterized for KIR3DL1*005 (35). Analysis of mRNA expression from sorted KIR3DL1 populations on primary cells from a heterozygous *KIR3DL1*001/*009* individual revealed that transcription of *KIR3DL1*001* and *KIR3DL1*009* segregated into two distinct populations defined by their KIR3DL1 surface phenotype. This segregation of KIR3DL1 allele expression at the transcript level supports previous studies that have demonstrated allele specific gene expression of KIR3DL1 (42, 43). Site directed mutagenesis of the wild-type KIR3DL1*001 revealed a glycine residue at the amino acid position 58 is the main contributor to KIR3DL1*009 phenotype, while a methionine residue at position 92 is necessary to completely reproduce the reduced surface expression phenotype of KIR3DL1*009. The higher conformational freedom of glycine at this position may increase the flexibility of the polypeptide chain, causing greater difficulty to properly fold and mature the receptor, ultimately resulting in intracellular retention of the receptor. Consistent with this interpretation, the surface expression of KIR3DL1*009 was enhanced to levels similar to KIR3DL1*001 on cells cultured at sub-physiological temperatures. These data are analogous to previous findings for KIR3DL1*004, which is completely retained within the ER at physiological temperatures but is capable of surface expression at reduced temperatures (39). We also observed that once at the cell surface, the stability of KIR3DL1*001 and KIR3DL1*009 was similar. Taken together, these results suggest KIR3DL1*009, similar to KIR3DL1*004, is likely retained within the cell caused by the presence of a glycine and methionine at amino acid positions 58 and 92.

The KIR3DS1 specific D0 polymorphisms also disrupted the interaction between KIR3DL1 and HLA-Bw4. The data presented within this manuscript identify two novel polymorphisms at position 58 (S58G) and 92 (V92M) that, in combination, cause a significant reduction in the capacity of KIR3DL1 to interact with HLA. Varying from the surface expression data, the methionine at position 92 is the key residue while the glycine at position 58 further augments the effect. Although amino acid position 92 does not directly interact with HLA, molecular dynamic analysis indicates that 92M causes steric hindrance within the molecule, resulting in a significant conformational shift within the D1 domain of KIR3DL1*009. This conformational shift significantly displaces the D1 domain amino acid residues that directly interact with HLA. Although prior investigations have shown an enhancer effect of the D0 domain (31, 44), our findings are the first to show that natural polymorphisms within this domain are sufficient to significantly reduce HLA binding. In

combination with the D1 polymorphisms of KIR3DS1*013, the effects imparted by the D0 polymorphisms provide the molecular mechanism by which KIR3DS1*013 has lost the ability to interact with HLA (20). The loss of ligand binding of KIR3DL1*009 and KIR3DL1*042 may have provided a protective effect in regions where pathogens caused an increase in the strength of the interaction between KIR3DL1 and HLA causing less NK cell mediated killing of the pathogen similar to evasive mechanisms described for HIV-specific peptides and inhibitory KIR function (45).

KIR3DL1*009 positive NK cells showed a greater capability of response against a HLA-B*44:03 positive target cell compared to KIR3DL1*001 or KIR3DL1*005 positive NK cells, suggesting that they have a weak sensitivity for inhibition. Given that KIR3DL1*009 is expressed at a surface density similar to KIR3DL1*005, the reduced ligand binding, rather than the reduced surface expression contributed to the lack of inhibition imparted by HLA-B*44:03. Although the inhibition observed for KIR3DL1*001 and KIR3DL1*005 positive NK cells was similar, this could be explained by the significantly greater strength of interaction observed between KIR3DL1*005 and HLA-B*44:03. It is therefore possible that the reduced surface expression of KIR3DL1*005 and other KIR3DL1 alleles may impact the functional capacity of the receptors when confronted with an HLA Bw4 antigen that exhibits weaker binding strength.

This study illuminates key functional effects on ligand recognition and receptor surface expression caused by D0 polymorphisms that are conserved in all KIR3DS1 alleles and are present in KIR3DL1*009, KIR3DL1*042, and KIR3DL1*057. The data presented further demonstrate the complexity of the KIR3DL1/HLA interaction and provides insight to how KIR3DL1 and HLA combinations may impact NK cell responses to viral pathogens and malignant cells.

Supplementary Material

Refer to Web version on PubMed Central for supplementary material.

Acknowledgments

The authors thank Jean-Benoit Le Ludeuc, Christopher Forlenza, Xia-Rong Liu, and Frances Weis-Garcia for technical assistance. We also thank Addgene for providing the pcDNA3-Clover vector from Dr. Michael Lin.

References

1. Carson WE, Fehniger TA, Caligiuri MA. CD56bright natural killer cell subsets: characterization of distinct functional responses to interleukin-2 and the c-kit ligand. European journal of immunology. 1997; 27:354–360. [PubMed: 9045904]
2. Cooper MA, Fehniger TA, Turner SC, Chen KS, Ghaheri BA, Ghayur T, Carson WE, Caligiuri MA. Human natural killer cells: a unique innate immunoregulatory role for the CD56(bright) subset. Blood. 2001; 97:3146–3151. [PubMed: 11342442]
3. Schleinitz N, March ME, Long EO. Recruitment of activation receptors at inhibitory NK cell immune synapses. PloS one. 2008; 3:e3278. [PubMed: 18818767]
4. Karre K, Ljunggren HG, Piontek G, Kiessling R. Selective rejection of H-2-deficient lymphoma variants suggests alternative immune defence strategy. Nature. 1986; 319:675–678. [PubMed: 3951539]

5. Ljunggren HG, Karre K. In search of the 'missing self': MHC molecules and NK cell recognition. Immunology today. 1990; 11:237–244. [PubMed: 2201309]
6. Cohen GB, Gandhi RT, Davis DM, Mandelboim O, Chen BK, Strominger JL, Baltimore D. The selective downregulation of class I major histocompatibility complex proteins by HIV-1 protects HIV-infected cells from NK cells. Immunity. 1999; 10:661–671. [PubMed: 10403641]
7. Le Gall S, Erdtmann L, Benichou S, Berlioz-Torrent C, Liu L, Benarous R, Heard JM, Schwartz O. Nef interacts with the mu subunit of clathrin adaptor complexes and reveals a cryptic sorting signal in MHC I molecules. Immunity. 1998; 8:483–495. [PubMed: 9586638]
8. Colonna M, Borsellino G, Falco M, Ferrara GB, Strominger JL. HLA-C is the inhibitory ligand that determines dominant resistance to lysis by NK1- and NK2-specific natural killer cells. Proceedings of the National Academy of Sciences of the United States of America. 1993; 90:12000–12004. [PubMed: 8265660]
9. Moretta A, Vitale M, Bottino C, Orengo AM, Morelli L, Augugliaro R, Barbaresi M, Ciccone E, Moretta L. P58 molecules as putative receptors for major histocompatibility complex (MHC) class I molecules in human natural killer (NK) cells. Anti-p58 antibodies reconstitute lysis of MHC class I-protected cells in NK clones displaying different specificities. The Journal of experimental medicine. 1993; 178:597–604. [PubMed: 8340759]
10. Winter CC, Gumperz JE, Parham P, Long EO, Wagtmann N. Direct binding and functional transfer of NK cell inhibitory receptors reveal novel patterns of HLA-C allotype recognition. Journal of immunology. 1998; 161:571–577.
11. Burshtyn DN, Scharenberg AM, Wagtmann N, Rajagopalan S, Berrada K, Yi T, Kinet JP, Long EO. Recruitment of tyrosine phosphatase HCP by the killer cell inhibitor receptor. Immunity. 1996; 4:77–85. [PubMed: 8574854]
12. Olcese L, Lang P, Vely F, Cambiaggi A, Marguet D, Blery M, Hippen KL, Biassoni R, Moretta A, Moretta L, Cambier JC, Vivier E. Human and mouse killer-cell inhibitory receptors recruit PTP1C and PTP1D protein tyrosine phosphatases. Journal of immunology. 1996; 156:4531–4534.
13. Anfossi N, Andre P, Guia S, Falk CS, Roetynck S, Stewart CA, Breso V, Frassati C, Reviron D, Middleton D, Romagne F, Ugolini S, Vivier E. Human NK cell education by inhibitory receptors for MHC class I. Immunity. 2006; 25:331–342. [PubMed: 16901727]
14. Liao NS, Bix M, Zijlstra M, Jaenisch R, Raulet D. MHC class I deficiency: susceptibility to natural killer (NK) cells and impaired NK activity. Science. 1991; 253:199–202. [PubMed: 1853205]
15. Parham P, Norman PJ, Abi-Rached L, Guethlein LA. Variable NK cell receptors exemplified by human KIR3DL1/S1. Journal of immunology. 2011; 187:11–19.
16. Single RM, Martin MP, Gao X, Meyer D, Yeager M, Kidd JR, Kidd KK, Carrington M. Global diversity and evidence for coevolution of KIR and HLA. Nature genetics. 2007; 39:1114–1119. [PubMed: 17694058]
17. Cella M, Longo A, Ferrara GB, Strominger JL, Colonna M. NK3-specific natural killer cells are selectively inhibited by Bw4-positive HLA alleles with isoleucine 80. The Journal of experimental medicine. 1994; 180:1235–1242. [PubMed: 7931060]
18. Gumperz JE, Litwin V, Phillips JH, Lanier LL, Parham P. The Bw4 public epitope of HLA-B molecules confers reactivity with natural killer cell clones that express NKB1, a putative HLA receptor. The Journal of experimental medicine. 1995; 181:1133–1144. [PubMed: 7532677]
19. Stern M, Ruggeri L, Capanni M, Mancusi A, Velardi A. Human leukocyte antigens A23, A24, and A32 but not A25 are ligands for KIR3DL1. Blood. 2008; 112:708–710. [PubMed: 18502829]
20. O'Connor GM, Yamada E, Rampersaud A, Thomas R, Carrington M, McVicar DW. Analysis of binding of KIR3DS1*014 to HLA suggests distinct evolutionary history of KIR3DS1. Journal of immunology. 2011; 187:2162–2171.
21. Boudreau JE, Le Luduec JB, Hsu KC. Development of a novel multiplex PCR assay to detect functional subtypes of KIR3DL1 alleles. PloS one. 2014; 9:e99543. [PubMed: 24919192]
22. Norman PJ, Abi-Rached L, Gendzekhadze K, Hammond JA, Moesta AK, Sharma D, Graef T, McQueen KL, Guethlein LA, Carrington CV, Chandanayingyong D, Chang YH, Crespi C, Saruhan-Direskeneli G, Hameed K, Kamkamidze G, Koram KA, Layrisse Z, Matamoros N, Mila J, Park MH, Pitchappan RM, Ramdath DD, Shiau MY, Stephens HA, Struik S, Tyan D, Verity DH, Vaughan RW, Davis RW, Fraser PA, Riley EM, Ronaghi M, Parham P. Meiotic

recombination generates rich diversity in NK cell receptor genes, alleles, and haplotypes. Genome research. 2009; 19:757–769. [PubMed: 19411600]

23. Lam AJ, St-Pierre F, Gong Y, Marshall JD, Cranfill PJ, Baird MA, McKeown MR, Wiedenmann J, Davidson MW, Schnitzer MJ, Tsien RY, Lin MZ. Improving FRET dynamic range with bright green and red fluorescent proteins. Nature methods. 2012; 9:1005–1012. [PubMed: 22961245]
24. Steiner NK, Dakshanamurthy S, VandenBussche CJ, Hurley CK. Extracellular domain alterations impact surface expression of stimulatory natural killer cell receptor KIR2DS5. Immunogenetics. 2008; 60:655–667. [PubMed: 18682925]
25. Hsu KC, Liu XR, Selvakumar A, Mickelson E, O'Reilly RJ, Dupont B. Killer Ig-like receptor haplotype analysis by gene content: evidence for genomic diversity with a minimum of six basic framework haplotypes, each with multiple subsets. Journal of immunology. 2002; 169:5118–5129.
26. Vilches C, Castano J, Gomez-Lozano N, Estefania E. Facilitation of KIR genotyping by a PCR-SSP method that amplifies short DNA fragments. Tissue antigens. 2007; 70:415–422. [PubMed: 17854430]
27. Hou L, Chen M, Steiner N, Kariyawasam K, Ng J, Hurley CK. Killer cell immunoglobulin-like receptors (KIR) typing by DNA sequencing. Methods in molecular biology. 2012; 882:431–468. [PubMed: 22665249]
28. Mulrooney TJ, Posch PE, Hurley CK. DAP12 impacts trafficking and surface stability of killer immunoglobulin-like receptors on natural killer cells. Journal of leukocyte biology. 2013; 94:301–313. [PubMed: 23715743]
29. Frazier WR, Steiner N, Hou L, Dakshanamurthy S, Hurley CK. Allelic variation in KIR2DL3 generates a KIR2DL2-like receptor with increased binding to its HLA-C ligand. Journal of immunology. 2013; 190:6198–6208.
30. Hilton HG, Vago L, Older Aguilar AM, Moesta AK, Graef T, Abi-Rached L, Norman PJ, Guethlein LA, Fleischhauer K, Parham P. Mutation at positively selected positions in the binding site for HLA-C shows that KIR2DL1 is a more refined but less adaptable NK cell receptor than KIR2DL3. Journal of immunology. 2012; 189:1418–1430.
31. Vivian JP, Duncan RC, Berry R, O'Connor GM, Reid HH, Beddoe T, Gras S, Saunders PM, Olshina MA, Widjaja JM, Harpur CM, Lin J, Maloveste SM, Price DA, Lafont BA, McVicar DW, Clements CS, Brooks AG, Rossjohn J. Killer cell immunoglobulin-like receptor 3DL1-mediated recognition of human leukocyte antigen B. Nature. 2011; 479:401–405. [PubMed: 22020283]
32. Bowers KJ, Chow E, Xu H, Dror RO, Eastwood MP, Gregersen BA, Klepeis JL, Kolossvary I, Moraes MA, Sacerdoti FD, Salmon JK, Shan Y, Shaw DE. Scalable algorithms for molecular dynamics simulations on commodity clusters. Proceedings of the 2006 ACM/IEEE Conference on Supercomputing. 2006
33. Gardiner MM, Guethlein LA, Shilling HG, Pando M, Carr WH, Rajalingam R, Vilches C, Parham P. Different NK cell surface phenotypes defined by the DX9 antibody are due to KIR3DL1 gene polymorphism. Journal of immunology. 2001; 166:2992–3001.
34. Tao SD, He YM, Ying YL, He J, Zhu FM, Lv HJ. KIR3DL1 genetic diversity and phenotypic variation in the Chinese Han population. Genes and immunity. 2014; 15:8–15. [PubMed: 24173144]
35. Yawata M, Yawata N, Draghi M, Little AM, Partheniou F, Parham P. Roles for HLA and KIR polymorphisms in natural killer cell repertoire selection and modulation of effector function. The Journal of experimental medicine. 2006; 203:633–645. [PubMed: 16533882]
36. Pando MJ, Gardiner CM, Gleimer M, McQueen KL, Parham P. The protein made from a common allele of KIR3DL1 (3DL1*004) is poorly expressed at cell surfaces due to substitution at positions 86 in Ig domain 0 and 182 in Ig domain 1. Journal of immunology. 2003; 171:6640–6649.
37. VandenBussche CJ, Dakshanamurthy S, Posch PE, Hurley CK. A single polymorphism disrupts the killer Ig-like receptor 2DL2/2DL3 D1 domain. Journal of immunology. 2006; 177:5347–5357.
38. VandenBussche CJ, Mulrooney TJ, Frazier WR, Dakshanamurthy S, Hurley CK. Dramatically reduced surface expression of NK cell receptor KIR2DS3 is attributed to multiple residues throughout the molecule. Genes and immunity. 2009; 10:162–173. [PubMed: 19005473]
39. Taner SB, Pando MJ, Roberts A, Schellekens J, Marsh SG, Malmberg KJ, Parham P, Brodsky FM. Interactions of NK cell receptor KIR3DL1*004 with chaperones and conformation-specific

antibody reveal a functional folded state as well as predominant intracellular retention. Journal of immunology. 2011; 186:62–72.

40. O'Connor GM, Vivian JP, Widjaja JM, Bridgeman JS, Gostick E, Lafont BA, Anderson SK, Price DA, Brooks AG, Rossjohn J, McVicar DW. Mutational and structural analysis of KIR3DL1 reveals a lineage-defining allotypic dimorphism that impacts both HLA and peptide sensitivity. Journal of immunology. 2014; 192:2875–2884.
41. Norman PJ, Abi-Rached L, Gendzekhadze K, Korbel D, Gleimer M, Rowley D, Bruno D, Carrington CV, Chandanayingyong D, Chang YH, Crespi C, Saruhan-Direskeneli G, Fraser PA, Hameed K, Kamkamidze G, Koram KA, Layrisse Z, Matamoros N, Mila J, Park MH, Pitchappan RM, Ramdath DD, Shiau MY, Stephens HA, Struik S, Verity DH, Vaughan RW, Tyan D, Davis RW, Riley EM, Ronaghi M, Parham P. Unusual selection on the KIR3DL1/S1 natural killer cell receptor in Africans. Nature genetics. 2007; 39:1092–1099. [PubMed: 17694054]
42. Chan HW, Kurago ZB, Stewart CA, Wilson MJ, Martin MP, Mace BE, Carrington M, Trowsdale J, Lutz CT. DNA methylation maintains allele-specific KIR gene expression in human natural killer cells. The Journal of experimental medicine. 2003; 197:245–255. [PubMed: 12538663]
43. Trundley A, Frebel H, Jones D, Chang C, Trowsdale J. Allelic expression patterns of KIR3DS1 and 3DL1 using the Z27 and DX9 antibodies. European journal of immunology. 2007; 37:780–787. [PubMed: 17301953]
44. Khakoo SI, Geller R, Shin S, Jenkins JA, Parham P. The D0 domain of KIR3D acts as a major histocompatibility complex class I binding enhancer. The Journal of experimental medicine. 2002; 196:911–921. [PubMed: 12370253]
45. Fadda L, Korner C, Kumar S, van Teijlingen NH, Piechocka-Trocha A, Carrington M, Altfeld M. HLA-Cw*0102-restricted HIV-1 p24 epitope variants can modulate the binding of the inhibitory KIR2DL2 receptor and primary NK cell function. PLoS pathogens. 2012; 8:e1002805. [PubMed: 22807681]

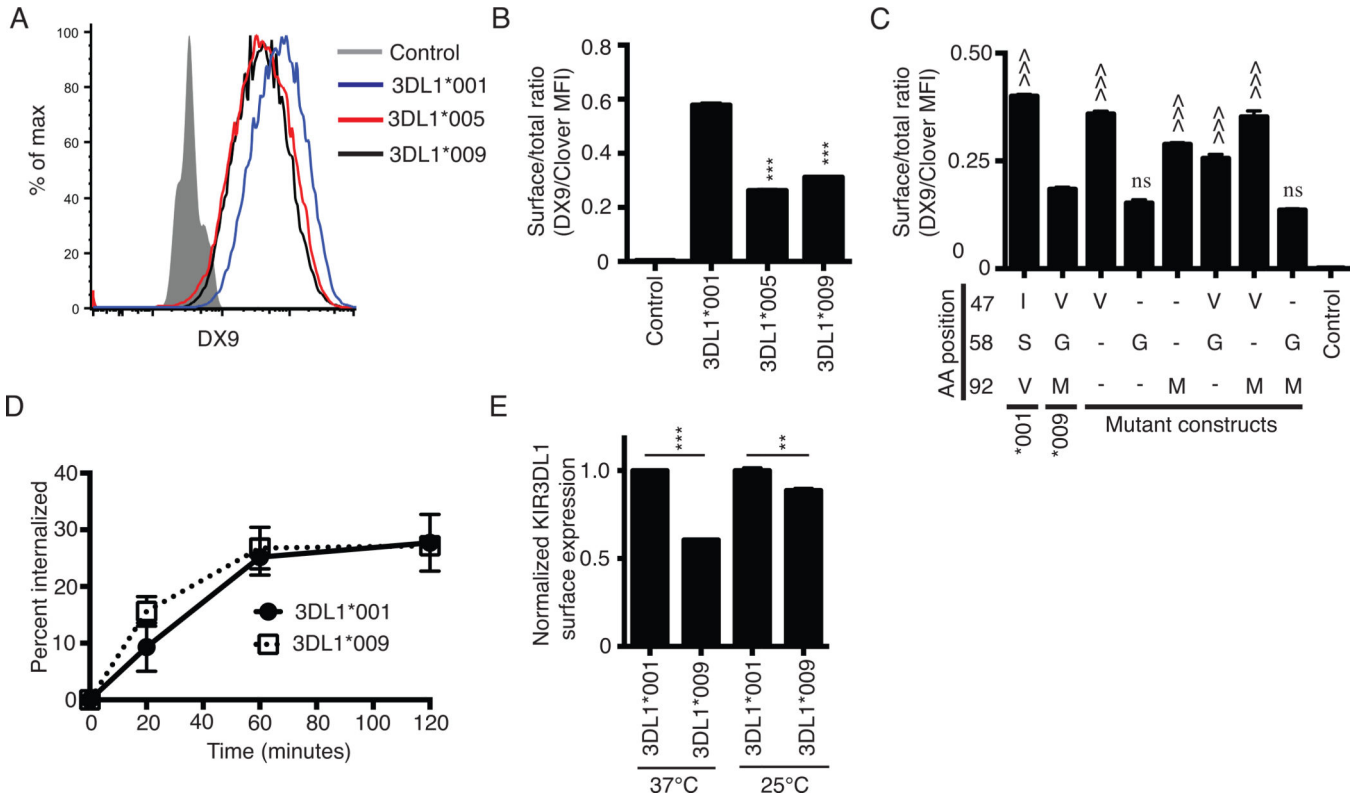

Figure 1.

KIR3DL1*009 is expressed at a low surface density. A, Flow cytometry histogram of KIR3DL1 surface expression on HEK293T cells following transfection with the C-terminally Clover tagged constructs encoding the alleles, KIR3DL1*001 (blue), KIR3DL1*005 (red), or KIR3DL1*009 (black). Surface expression was detected on Clover positive cells using the KIR3DL1 specific antibody, DX9. HEK293T cells transfected with the construct encoding KIR3DL1*001 and stained with an isotype control antibody were used as the negative control (filled grey histogram). B, KIR3DL1 surface expression from panel A presented as a ratio of surface expressed KIR (DX9 MFI) to total KIR expression (Clover MFI). C, KIR3DL1 cell surface expression ratios following transfection of HEK293T cells with wild-type KIR3DL1*001, KIR3DL1*009, or mutant constructs of KIR3DL1*001. As in panel B, the data are presented as a ratio of surface expression (DX9 MFI) to total expression (Clover MFI). Dashes represent amino acids that are the same as KIR3DL1*001 at the respective position. D, Internalization of KIR3DL1*001 (closed circle) and KIR3DL1*009 (open square) was monitored on transfected HEK293T cells following incubation at 37°C with PE-conjugated DX9 for indicated time points. E, KIR3DL1 surface expression on HEK293T cells transfected with KIR3DL1*001 (dashed black line) or KIR3DL1*009 (solid black line) following culture at either 37°C or 25°C. Surface expression was detected on Clover positive cells using DX9. The KIR3DL1 surface expression ratios are normalized to the ratio obtained for KIR3DL1*001 at each temperature independently. All experiments were performed in triplicate and reproduced in three independent experiments. The data from panels B and C were analyzed by one-way ANOVA followed by a Tukey's multiple comparisons test. The data for each temperature in

panel E were analyzed independently using an unpaired Student's t-test (vs. KIR3DL1*001, *** P<0.001; vs. KIR3DL1*009, ^^^ P<0.001; ns, not significant).

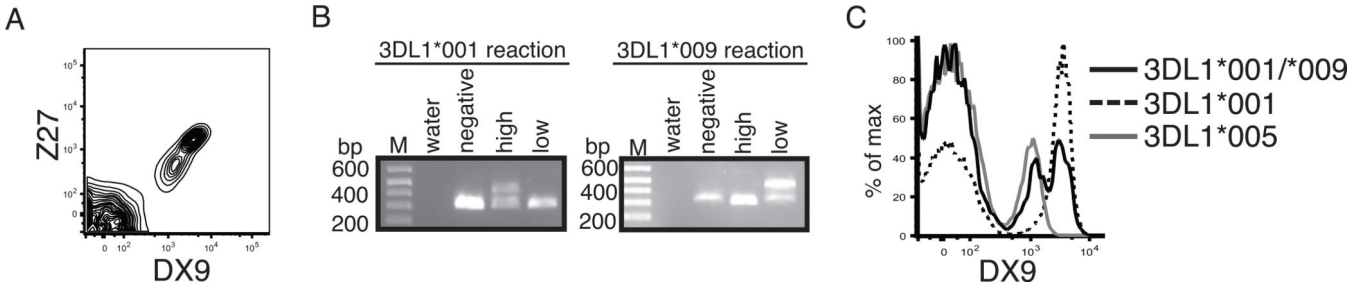

Figure 2.

KIR3DL1*009 segregates to a low density population on primary NK cells. A, Representative KIR3DL1 surface expression on the surface of primary NK cells (CD56+, CD3−) from a heterozygous KIR3DL1*001/*009 positive individual as detected by DX9 and Z27. B, RT-PCR amplification of KIR3DL1*001 (left panel) and KIR3DL1*009 (right panel) from sorted KIR3DL1 negative, low density, and high density populations. The lower and higher bands are the control and KIR specific amplicons, respectively. Representative flow cytometry histogram of KIR3DL1 surface expression on NK cells from individuals who express KIR3DL1*001 and KIR3DL1*009 (black, n=2), KIR3DL1*001 only (dashed, n=3), or KIR3DL1*005 only (grey, n=3).

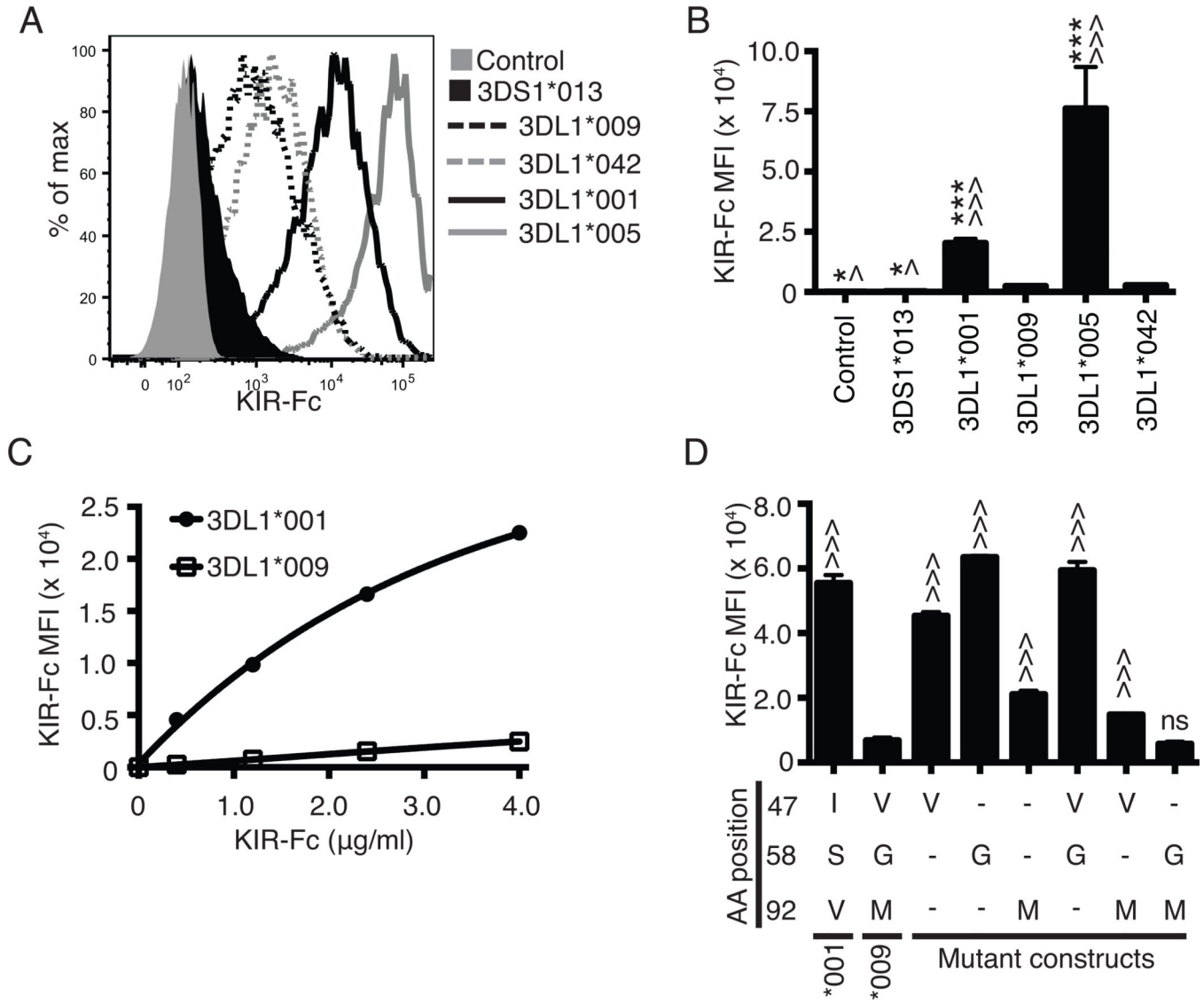

Figure 3.

Combined polymorphisms at amino acid positions 58 and 92 disrupt binding capacity of KIR3DL1 to HLA-B*44:03. A, Flow cytometry was used to assess 4.0 µg/ml of KIR3DL1*001-Fc (solid black line), KIR3DL1*009-Fc (dashed black line), KIR3DL1*005 (solid grey line), KIR3DL1*042 (dashed grey) or KIR3DS1*013-Fc (filled black line) binding to HLA-B*44:03 on the surface of 721.221 cells. Probing of the HLA class I negative parental 721.221 cells with KIR3DL1*001-Fc was used as the negative control (filled grey histogram). The amount of KIR-Fc binding was detected via flow cytometry using a PE-conjugated antibody specific for human IgG (KIR-Fc MFI). B, The MFI values obtained for the amount of PE secondary antibody binding (KIR-Fc MFI) represent the quantity of KIR-Fc protein binding from panel A. C, MFI values following flow cytometry analysis of binding of KIR3DL1*001-Fc (closed circle) and KIR3DL1*009-Fc (open square) to HLA-B*44:03 on 721.221 cells are presented for a concentration gradient of soluble KIR-Fc concentrations (0.4 – 4.0 µg/ml). D, Displayed are the MFI values

representing binding of each KIR-Fc protein (4.0 μg/ml) to HLA-B*44:03 on 721.221 cells as detected by a PE-conjugated secondary antibody. Dashes represent amino acids that are the same as KIR3DL1*001 at the respective position. All experiments were performed in triplicate and repeated in three independent experiments. The data were analyzed by one-way ANOVA followed by a Tukey's multiple comparisons test (vs 3DL1*009-Fc, ^ $P < 0.05$, ^^^ $P < 0.001$; vs. KIR3DL1*042, * $P < 0.05$, *** $P<0.001$; ns, not significant).

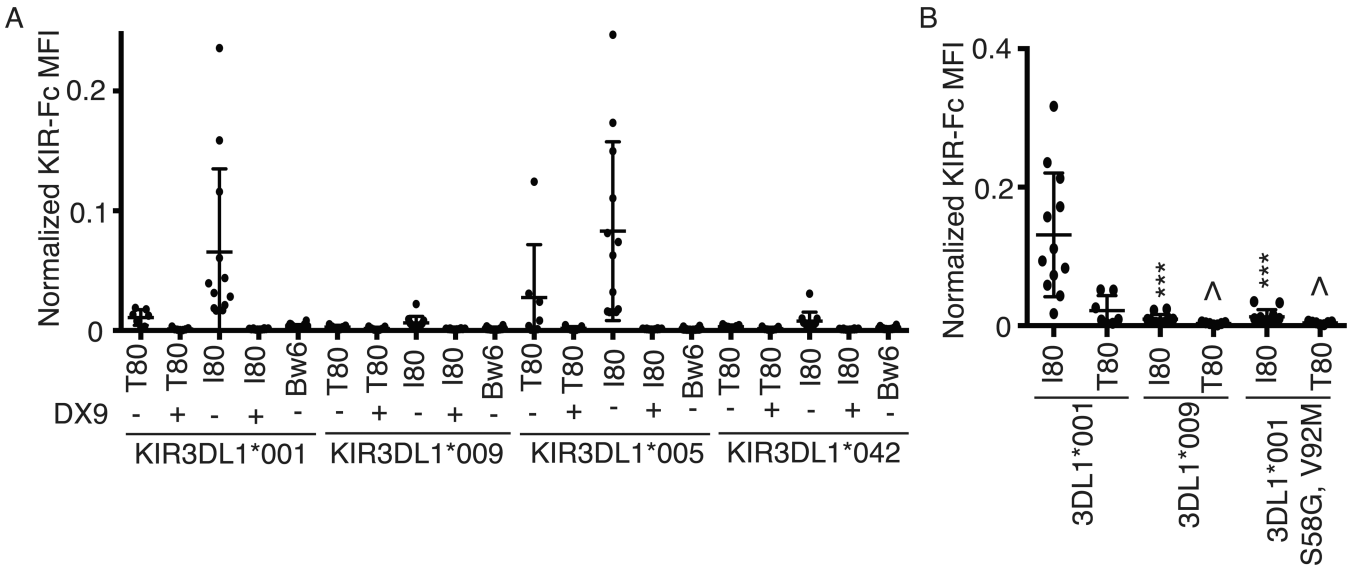

Figure 4.

KIR3DL1*009 binds poorly to a panel of HLA-Bw4 antigens. A, Soluble KIR-Fc (4.0 μg/ml) binding to a panel of 12 HLA Bw4 80I antigens, 6 HLA Bw4 80T and 31 HLA Bw6 antigens was assessed using a bead-based multiplex platform. Each data point represents binding levels to an individual HLA molecule. The binding was performed in the presence or absence of DX9 as indicated. B, Soluble wild-type KIR3DL1*001 and KIR3DL1*009 binding to a multiplex of HLA antigens was compared to the binding of the mutant, KIR3DL1*001 S58G, V92M. The data are presented as a normalized ratio accounting for the total amount of HLA conjugated to each bead as described in the methods section. These experiments were performed in triplicate and repeated in three independent experiments. The data were analyzed by one-way ANOVA followed by a Tukey's multiple comparisons test (vs 3DL1*001-Fc, * $P < 0.05$, *** $P < 0.001$).

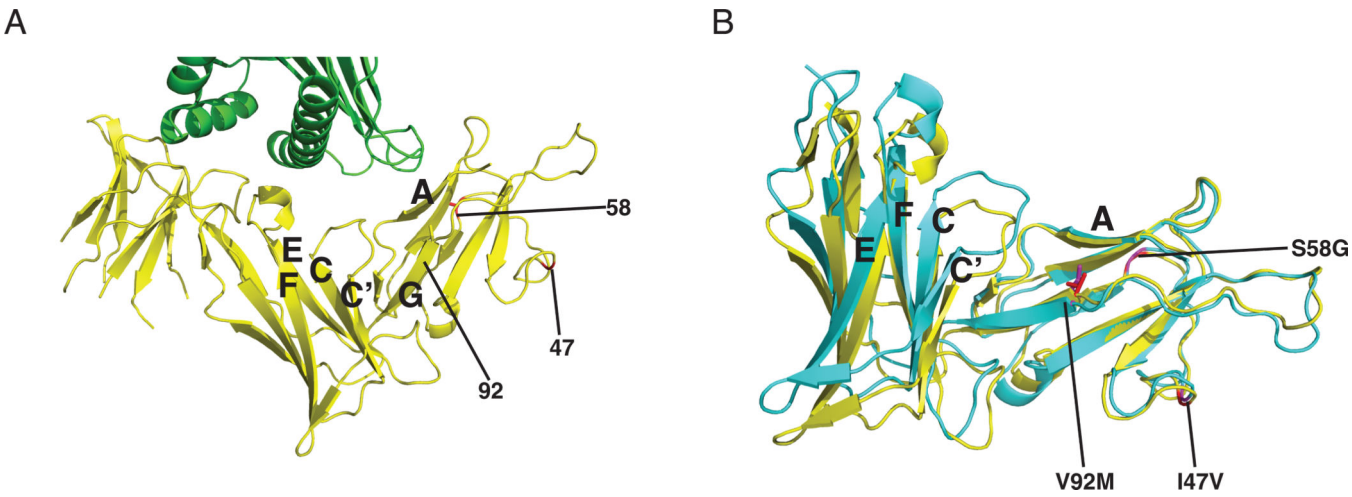

Figure 5.

Molecular dynamic simulation proposes a conformational shift in KIR3DL1*009 caused by 92M. A, Shown is a cartoon representation of the D0 and D1 domains of KIR3DL1*001 (yellow) interacting with HLA-B*57:01 (green) (31). The locations of the KIR3DL1*009 polymorphisms are marked as red in the structure and identified by number. The letters correspond to the strands of interest of the D0 (A, G) and D1 (C, C', E, F) domains. B, Displayed is an overlay of the predicted molecular structure of KIR3DL1*009 (blue-green) with the crystal structure of KIR3DL1*001 (yellow) following molecular dynamic simulation. The side chains of valine of KIR3DL1*001 (red) and methionine of KIR3DL1*009 (purple) at position 92 are displayed while positions 47 and 58 are identified by color and number.

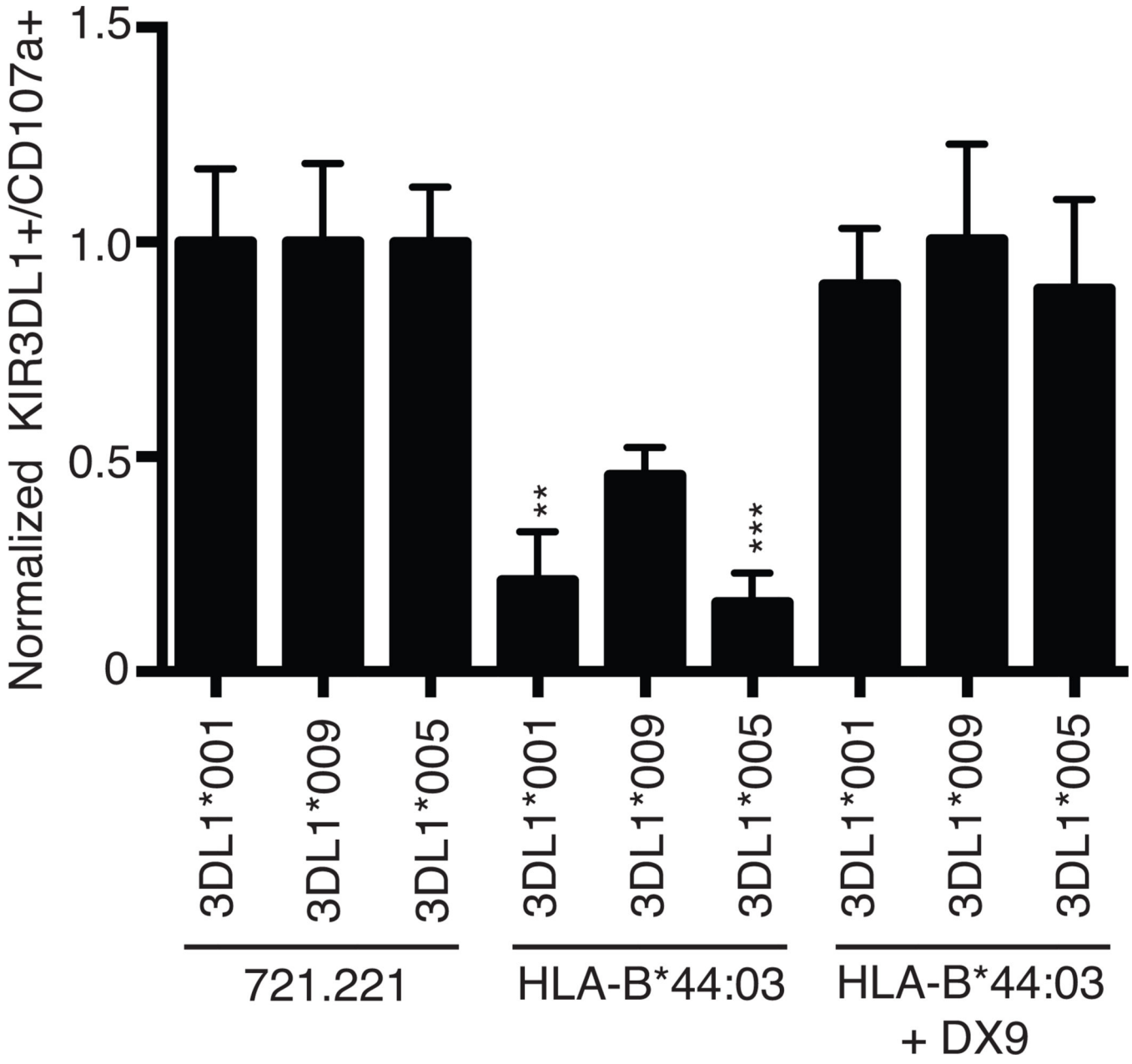

Figure 6.

KIR3DL1*009 positive NK cells exhibit greater response to HLA-Bw4 positive target cells. PBMCs from a healthy donor heterozygous for *KIR3DL1*001* and *KIR3DL*009* as well as PBMCs from a *KIR3DL1*005* positive donor were challenged with HLA negative 721.221 cells or 721.221 cells expressing HLA-B*44:03 in the presence or absence of the blocking DX9 antibody. Activation was determined independently for each KIR3DL1 positive population using Z27. The responses for each KIR3DL1 population were normalized to activation observed for each population after co-incubation with the parental 721.221 cells. These experiments were performed in triplicate and repeated in three independent

experiments. The results were analyzed using a one-way ANOVA followed by a Tukey's multiple comparisons test (vs 3DL1*009, ** $P < 0.01$, *** $P < 0.001$; ns, not significant).

Table I

Amino acid polymorphisms within the D0 extracellular domain of KIR3DL1 between KIR3DL1*001, KIR3DL1*009, KIR3DL1*005, KIR3DL1*042 and KIR3DS1*013.

	D0 domain polymorphisms (Amino acid position)		
Allele	**47**	**58**	**92**
KIR3DL1*001	I	S	V
KIR3DL1*009	V	G	M
KIR3DS1*013	V	G	M
KIR3DL1*005	I	S	V
KIR3DS1*042	V	G	M